HAL
archives-ouvertes.fr

Angular Talbot effect

José Azaña, Hugues Guillet de Chatellus

▶ **To cite this version:**

José Azaña, Hugues Guillet de Chatellus. Angular Talbot effect. Physical Review Letters, American Physical Society, 2014, pp.112-213902-1 à 112-213902-5. <10.1103/PhysRevLett.112.213902>. <hal-00998967>

HAL Id: hal-00998967
https://hal.archives-ouvertes.fr/hal-00998967

Submitted on 3 Jun 2014

HAL is a multi-disciplinary open access archive for the deposit and dissemination of scientific research documents, whether they are published or not. The documents may come from teaching and research institutions in France or abroad, or from public or private research centers.

L'archive ouverte pluridisciplinaire **HAL**, est destinée au dépôt et à la diffusion de documents scientifiques de niveau recherche, publiés ou non, émanant des établissements d'enseignement et de recherche français ou étrangers, des laboratoires publics ou privés.

Angular Talbot effect

José Azaña[1,*] and Hugues Guillet de Chatellus[2]
[1]INRS—Énergie, Matériaux et Télécommunications, Montréal, Québec H5A1K6, Canada
[2]Laboratoire Interdisciplinaire de Physique, CNRS—Université Joseph Fourier, UMR 5588, BP 87—38402 Saint Martin d'Héres, France
(Received 5 March 2014; published 29 May 2014)

We predict the possibility of observing integer and fractional self-imaging (Talbot) phenomena on the discrete angular spectrum of periodic diffraction gratings illuminated by a suitable spherical wave front. Our predictions are experimentally validated, reporting what we believe to be the first observation of self-imaging effects in the far-field diffraction regime.

DOI: 10.1103/PhysRevLett.112.213902 PACS numbers: 42.25.Fx, 42.30.Kq, 42.79.Dj

The Talbot effect, also referred to as self-imaging, is a concept with a distinguished pedigree [1–4]. The Talbot effect was first discovered and explained in the context of classical diffraction optics [1–3]. Moreover, the concept can be easily transferred to a wide variety of problems [4], which can be described using equivalent laws to those of the physics of diffraction of periodic wave fields [5], [6]. Manifestations of the effect have been observed and applied across many fundamental and applied areas, including waveguide devices [7], x-ray diffraction and imaging [8], electron microscopy [9], plasmonics [10], nonlinear dynamics [11], matter-wave interactions [12], laser physics [13], quantum mechanics [14,15], etc. Self-imaging of periodic temporal waveforms has been also reported in dispersive media [16]. Referring to its original optics description [1–3], Talbot phenomena can be observed when a coherent beam of monochromatic light is transmitted through a one-dimensional (1D) or two-dimensional (2D) periodic object, namely, a grating. Plane wave-front illumination is generally assumed. Following free-space diffraction, exact images of the original object are formed at specific distances from the object (integer Talbot). At other positions along the diffraction direction, the periodic pattern reappears but with a periodicity that is reduced by an integer number with respect to the input one (fractional Talbot). Similar self-imaging phenomena can be also observed using illumination with a Gaussian-like wave front [3,4]; in this case, the diffraction-induced "self-images" are transversally magnified or compressed versions of the original ones.

Regardless of their specific manifestation, Talbot phenomena are intrinsically near-field diffraction effects; i.e., they are the result of wave interference in the near-field diffraction region or equivalent regime [1–16]. Thus, it is generally accepted that these phenomena cannot be produced or observed under far-field or Fraunhofer diffraction conditions. In this Letter, we show, otherwise, that self-imaging can be induced on the angular spectrum of periodic gratings, i.e., on their far-field diffraction patterns. The key is to use illumination with a suitable parabolic wave front, e.g., a spherical wave front (point source) under the Fresnel approximation. We refer to this new class of self-imaging effects as "angular Talbot phenomena." We anticipate that both integer and fractional self-images of the original angular spectrum can be induced by properly fixing the curvature of the illumination beam, e.g., the distance between the source focal point and grating location. Our theoretical predictions are experimentally confirmed.

Figure 1 shows a scheme of the problem under analysis, illustrating the predicted angular Talbot effect. We assume a 1D grating illuminated by a coherent monochromatic beam of wavelength λ and associated wave number $k = 2\pi/\lambda$.

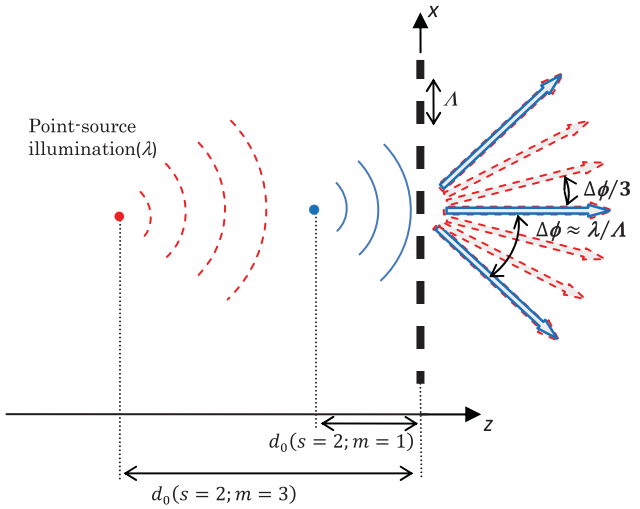

FIG. 1 (color). Schematic representation of angular Talbot phenomena observed by spherical wave-front illumination of a periodic diffraction grating. The detailed condition for d_0 depending on the integer parameters s and m is given in Eq. (6). The figure represents the cases of a direct, integer angular Talbot effect ($s = 2$; $m = 1$), whose diffraction is identical to the one found under plane wave-front illumination, and a direct, fractional angular Talbot effect ($s = 2$; $m = 3$), for which the same beams are diffracted with one-third of the separation angle $\Delta\phi$.

 © 2014 American Physical Society

The grating extends along the direction x, perpendicular to the light propagation direction z, with complex transmission amplitude defined by

$$t(x) = \sum_{p=-\infty}^{+\infty} t_p g(x - p\Lambda) = g(x) \circ [t_{\text{env}}(x) \sum_{p=-\infty}^{+\infty} \delta(x - p\Lambda)], \tag{1}$$

where $p = 0, \pm 1, \pm 2, \ldots$, $\circ$ denotes a convolution integral, Λ is the grating period, $g(x)$ is the complex-amplitude shape of the individual grating aperture, $\delta(x)$ is the Dirac delta, and $t_p = t_{\text{env}}(p\Lambda)$ is a complex parameter that accounts for amplitude and phase variations among consecutive apertures and the truncation associated to the finite grating length, i.e., the grating complex envelope $t_{\text{env}}(x)$.

We recall first the well-known case of illumination with a plane wave front [17], which is assumed to propagate along z. In this case, the field complex amplitude $e_1(x)$ at the grating location ($z = 0$) is proportional to the grating amplitude transmission in Eq. (1), and the corresponding angular spectrum can then be written as

$$\begin{aligned} E_1(k_x) &= \text{FT}\{e_1(x)\} \\ &\propto G(k_x) \sum_{q=-\infty}^{+\infty} T_{\text{env}}(k_x - qK_0) \\ &= \sum_{q=-\infty}^{+\infty} G_q T_{\text{env}}(k_x - qK_0), \end{aligned} \tag{2}$$

where the symbol $\propto$ expresses proportionality, FT holds for Fourier transform, $q = 0, \pm 1, \pm 2, \ldots$, $K_0 = 2\pi/\Lambda$, $G_q = G(qK_0)$, with $G(k_x) = \text{FT}\{g(x)\}$ and $T_{\text{env}}(k_x) = \text{FT}\{t_{\text{env}}(x)\}$. Equation (2) has been derived by applying well-known FT rules on Eq. (1), including the convolution-multiplication theorem and the periodic comb pair $\text{FT}\{\sum_{p=-\infty}^{+\infty} \delta(x - p\Lambda)\} \propto \sum_{q=-\infty}^{+\infty} \delta(k_x - qK_0)$ (see Ref. [17], Chap. 2). Additionally, the transversal width of $g(x)$ is assumed to be sufficiently short so that $G(k_x)$ is approximately constant along a frequency resolution given by the angular extension (bandwidth) of $T_{\text{env}}(k_x)$. Notice that the bandwidth of T_{env} scales as the inverse of the total grating length.

Equation (2) can be interpreted as a collection of monochromatic beams, each beam associated with a different diffraction order q and propagating with an angle ϕ_q with respect to the axis z, $\sin\phi_q = qK_0/k = q(\lambda/\Lambda)$. Moreover, all individual beams exhibit the same angular spectrum determined by the FT of the grating complex envelope $t_{\text{env}}(x)$, i.e., $T_{\text{env}}(k_x)$.

Our interest here focuses on the case of illumination of the same physical grating with a parabolic (quadratic-phase) wave front. We assume that the complex amplitude of the parabolic wave at the grating location ($z = 0$) is proportional to $\exp(j\alpha x^2)$, where $j = \sqrt{-1}$ is the imaginary unit, and α defines the curvature of the quadratic phase profile. Under the Fresnel approximation (see Ref. [17], Chap. 4), this wave variation can be practically induced by illumination with a spherical wave front, ideally generated from a single radiation point on the propagation axis ($x = 0$, $z = -d_0$), see Fig. 1. In this specific case, $\alpha = \pi/\lambda d_0$.

Under parabolic wave-front illumination, the wave complex amplitude $e'_1(x)$ at the grating location ($z = 0$) is now given by

$$\begin{aligned} e'_1(x) &\propto \exp(j\alpha x^2) \sum_{p=-\infty}^{+\infty} t_p g(x - p\Lambda) \\ &\approx \sum_{p=-\infty}^{+\infty} \exp(jp^2\alpha\Lambda^2) t_p g(x - p\Lambda) \end{aligned} \tag{3}$$

The latest approximation in Eq. (3) is valid if the transversal extension of the individual aperture $g(x)$ is sufficiently short [18]. Equation (3) resembles the equation that is obtained for the angular spectrum $E_2(k_x)$ of a grating illuminated by a plane wave front after free-space near-field diffraction, Eq. (4) below. In the classical grating diffraction case, the angularly equispaced diffracted beams (each approaching a plane wave and characterized by a different order q) are phase shifted with respect to each other following a parabolic phase-shift distribution ($\propto q^2$), as directly induced by the near-field (NF) diffraction process [3–6], [17]. Mathematically, the wave angular spectrum after diffraction through a distance d_{NF} is

$$E_2(k_x) \propto \sum_{q=-\infty}^{+\infty} \exp(jq^2K_0^2 d_{\text{NF}}/2k) G_q T_{\text{env}}(k_x - qK_0). \tag{4}$$

Equivalently, in the problem under consideration, the periodically spaced apertures of the diffraction grating behave as consecutive spherical-like wave-front beam sources (each characterized by a different p). Equation (3) implies that these beams are also phase shifted with respect to each other following a similar parabolic phase-shift distribution ($\propto p^2$). The mathematical equivalence between Eqs. (3) and (4) establishes a duality between the angular spectrum domain (k_x) in the conventional problem of diffraction of a periodic wave field, Eq. (4), and the transversal spatial domain (x) of a periodic grating under parabolic wave-front illumination, Eq. (3), and vice versa. This duality is central to our predictions on angular Talbot phenomena, as detailed in what follows.

The phase modulation induced by parabolic illumination, Eq. (3), generally alters the wave angular spectrum as compared with that obtained under plane wave-front illumination, Eq. (2). In line with the equivalence outlined

above, the distortions induced on the wave angular spectrum should follow a similar evolution to those observed for the transversal diffraction patterns in the standard periodic grating diffraction problem. Indeed, the central finding in our work is that the angular spectrum is modified in peculiar and distinctive ways when the following condition is satisfied on the discrete phase-modulation shifts in Eq. (3):

$$\alpha\Lambda^2 = \pi\frac{s}{m}, \tag{5}$$

where $s(=1,2,3,\ldots)$ and $m(=1,2,3,\ldots)$ are any two coprime integers. Equation (5) is derived as the counterpart of the general Talbot condition in the classical diffraction problem of periodic wave fields [6]. As such, Eq. (5) will be referred to as the angular Talbot condition. In the spherical wave-front implementation depicted in Fig. 1, Eq. (5) implies a condition on the location ($z = -d_0$) of the focal point of the spherical beam,

$$d_0(s;m) = \frac{m}{s}\frac{\Lambda^2}{\lambda} = \frac{m}{s}z_T, \tag{6}$$

where $z_T = \Lambda^2/\lambda$ will be referred to as the fundamental Talbot length.

Similar to its spatial counterpart [6], direct (inverted) and integer (fractional) Talbot phenomena can be observed on the angular spectrum of the wave amplitude, or the proportional far-field diffraction pattern, depending on the combination of values of the parameters s and m in Eq. (5). In particular, similar derivations to those previously reported for the spatial Talbot problem [3,6] allow us to predict that when condition (5) or the equivalent Eq. (6) is satisfied, then the angular spectrum of the diffracted wave can be written as follows:

$$E'_1(k_x) \propto \sum_{q=-\infty}^{+\infty} G_q T_{\text{env}}\left(k_x - q\frac{K_0}{m} - h\frac{K_0}{2m}\right), \tag{7}$$

where $h = 1$ if the product sm is an odd number and $h = 0$ if the product sm is an even number. According to Eq. (7), the following phenomena are possible.

(1) The case $m = 1$ corresponds to integer angular Talbot phenomena. The easiest case to interpret occurs when $m = 1$ and s is an even number ($s = 2,4,6,\ldots$). In this case, the condition in Eq. (5) implies that the phase-modulation shifts in Eq. (3) $p^2\alpha\Lambda^2$, are proportional to 2π for all values of p. As a result, the phase modulation induced by the parabolic illumination does not have any effect on the wave amplitude, and, consequently, the wave angular spectrum is similarly given by Eq. (2). This implies that the wave is diffracted exactly as in the case of illumination by a parallel plane wave front, as described above. This effect can be interpreted as the angular

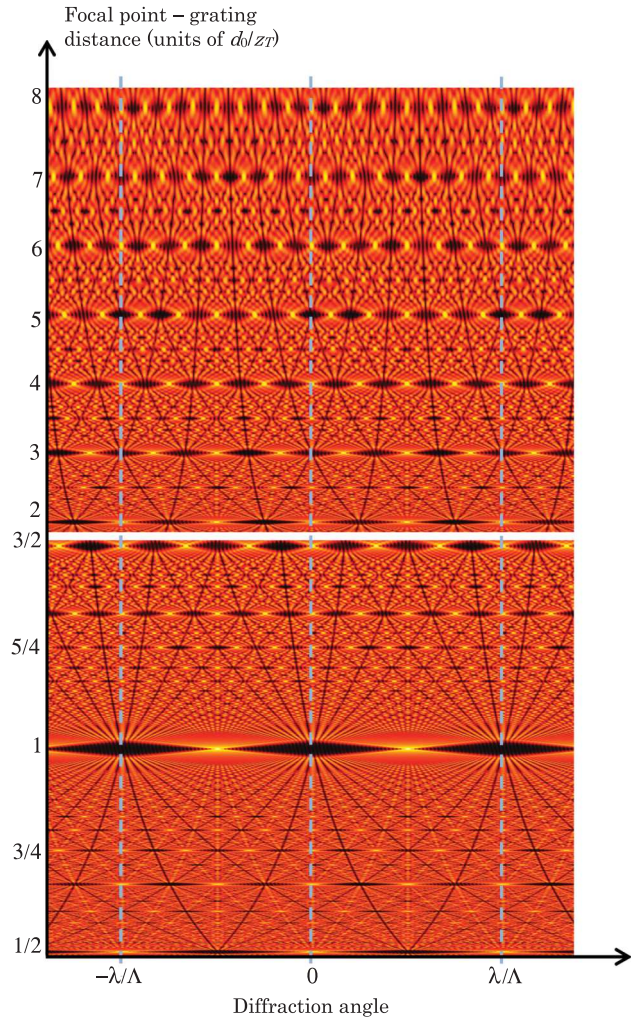

FIG. 2 (color). Theoretical angular Talbot carpet for a grating with $N = 40$ apertures. The carpet shows the evolution of the angular spectrum magnitude of the diffracted wave (versus the diffraction angle) as a function of the source focal point location with respect to the grating, normalized as d_0/z_T. Angular Talbot phenomena are observed when $d_0/z_T = m/s$, with m and s being coprime integers. The vertical dotted lines represent the directions of the diffracted beams when the grating is shined with a plane wave front.

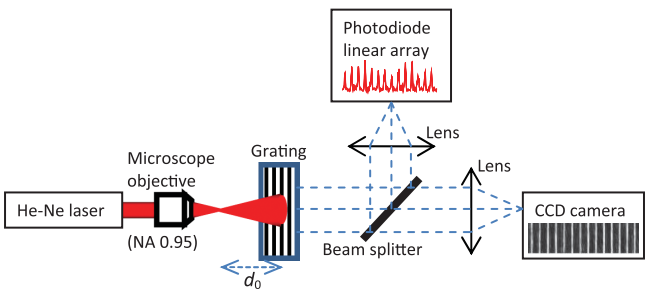

FIG. 3 (color). Sketch of the experimental setup.

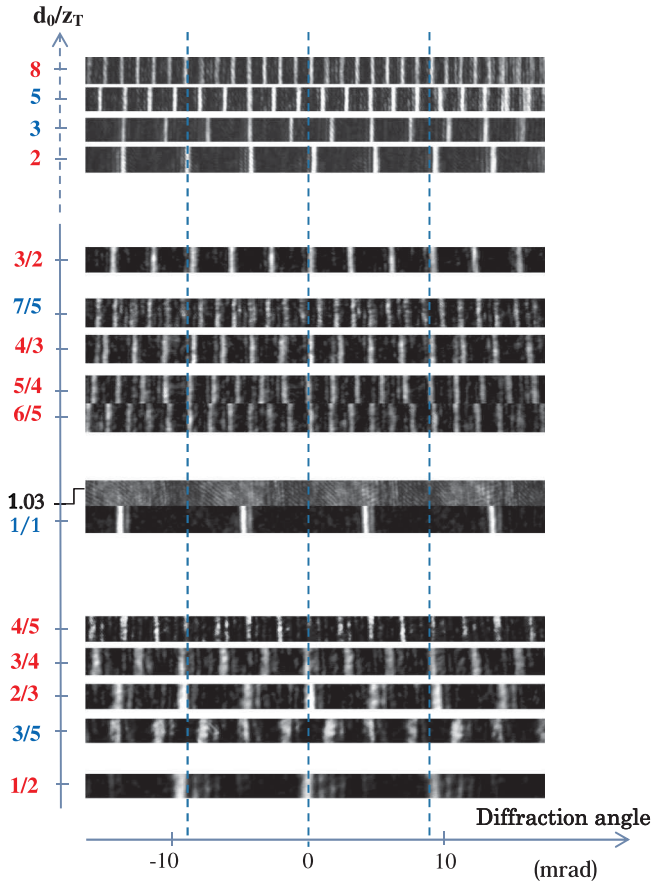

FIG. 4 (color). Experimental far-field diffraction patterns recorded with the CCD camera, as a function of the position of the pointlike source expressed in units of the Talbot length $z_T = \Lambda^2/\lambda$. Values of d_0 given in blue (respectively, red) correspond to inverted (respectively, direct) Talbot effects. The broadening of the diffracted beams when d_0 gets smaller than z_T is due to nonuniform illumination of the grating as the pointlike source approaches the grating. The vertical dashed lines represent the directions of the diffracted beams when the grating is shined with a plane wave front.

equivalent of a direct integer Talbot effect [1–4,6]. In contrast, for s odd (sm is odd), the beams are diffracted with the same periodic angular spacing but with an additional overall angular shift ϕ_0 defined by $\sin\phi_0 = K_o/2k = \lambda/2\Lambda$, namely, half the grating nominal diffraction angle. This latter case will be referred to as the inverted integer angular Talbot effect.

(2) When $m > 1$ ($m = 2, 3, 4, \ldots$), fractional angular Talbot phenomena are observed. The wave is again diffracted into a set of angularly dispersed beams, each with an individual angular spectrum that is identical to that obtained under plane wave-front illumination, but with an angular separation that is divided by a factor m with respect to the plane wave-front case. In particular, when the product (sm) is even, the diffraction angle for the beam of order q is now defined by $\sin\phi_q = qK_0/mk = q(\lambda/m\Lambda)$ (direct

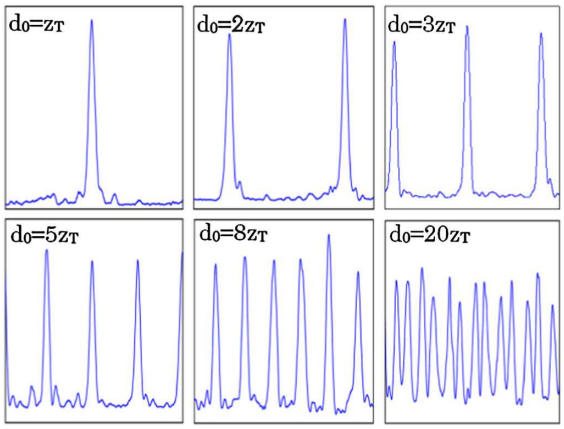

FIG. 5 (color online). Intensity profiles of the diffracted waves recorded by the PLA. The point source-grating distance is adjusted to satisfy the angular Talbot condition $d_0(s = 1; m) = m\Lambda^2/\lambda$, with $m = 1$, 2, 3, 5, 8, and 20 from left to right and top to bottom. The horizontal span of the PLA corresponds to a total angle aperture of 6 mrad. The FWHM widths of the diffraction peaks are measured to be 0.20 ± 0.02 mrad (for $m = 1$ to 8).

fractional angular Talbot effect). When the product (sm) is an odd number, one would observe an additional overall angular shift by ϕ_0, with $\sin\phi_0 = K_0/2mk = \lambda/2m\Lambda$, namely, half the reduced diffraction angle (inverted fractional angular Talbot effect).

Thus, under fractional angular Talbot conditions, the diffraction process is formally equivalent to that achieved when a plane wave is transmitted through a "virtual" periodic grating with a spatial period m times larger than the period of the actual physical grating. Through the described effect, the virtual grating period can be effectively controlled (e.g., increased) by simply shifting the point source location, according to condition (6), without affecting the total amount of energy transmitted through the grating.

The predicted fractional Talbot effects can be observed as long as there is no interference between consecutive diffracted beams. This implies that the diffraction-angle division factor m must remain in the limit where

$$T_{\mathrm{env}}(\pm K_0/2m) \to 0. \tag{8}$$

Figure 2 presents the numerically simulated angular Talbot carpet, clearly showing the different predicted angular Talbot phenomena.

Figure 3 shows an illustration of the used experimental setup. A He-Ne laser beam ($\lambda = 633$ nm) is sent onto a microscope objective (×100, 0.95 numerical aperture) to produce a pointlike light source. A grating of slits is placed on a translation stage, which enables a fine-tuning of the distance d_0 between the light beam focus and the grating. The grating is made of $N = 36$ vertical parallel slits (width:

7 μm, period Λ:70 μm). The light field at the grating output is then split by a 50:50 beam splitter and directed onto a CCD camera and a horizontal photodiode linear array (PLA), respectively. Both measurement systems are placed in the focal plane of two converging lenses, each with a focal length (f) of 20 cm. This scheme allows us to measure and record the angular spectrum or equivalent far-field diffraction pattern of the light diffracted from the grating, according to the well-known relationship between the angular frequency variable k_x and transversal direction variable x in the lens focal plane, $k_x = (k/f)x$ [17].

In our setup, the fundamental Talbot length z_T from Eq. (6) is equal to 7.8 mm. The distance d_0 between the focal point and the grating can be adjusted from $z_T/2$ up to $20z_T$. Figure 4 shows the patterns measured through a CCD camera, confirming observation of the predicted direct and inverted, integer and fractional self-imaging effects on the angular spectrum of the diffracted waves. Integer self-imaging is achieved when $m = 1$ (cases $d_0/z_T = 1/2$ and 1), and the expected division in the periodic spacing of the diffracted lines by a factor of m is clearly observed. Moreover, an example is also shown ($d_0 = 1.03\ z_T$, i.e., $m = 103$, $s = 100$) to illustrate how the periodic far-field diffraction patterns are severely distorted when the condition in Eq. (8) is not satisfied.

Finally, Fig. 5 displays the intensity measured by the PLA over 1.2 mm, for the cases when $s = 1$ and $m = 1$, 2, 3, 5, 8, and 20. These results confirm that the angular width of the different diffraction orders is nearly identical for all self-images, regardless of the induced angular-spacing division factor m, in agreement with our theoretical predictions. We recall that the angular width of the different diffraction orders is inversely proportional to the total grating length. Also, as predicted, when m is too large so that Eq. (8) is not satisfied, the diffracted beams begin to overlap, as illustrated in Fig. 5, bottom right.

In summary, this Letter reports the first theoretical prediction and experimental observation of integer and fractional self-imaging effects on the angular spectrum, or the far-field diffraction patterns, of periodic gratings illuminated by a suitable spherical wave front. This discovery should open the path for observation of related novel phenomena and new application opportunities across the wide range of disciplines where conventional (near-field) Talbot effects have been observed and successfully used.

*azana@emt.inrs.ca

[1] H. F. Talbot, Philos. Mag. **9**, 401 (1836).
[2] Lord Rayleigh, Philos. Mag. **11**, 196 (1881).
[3] K. Patorski, in *Progress in Optics*, edited by E. Wolf (North-Holland, Amsterdam, 1989), Vol. 27, pp. 1–108.
[4] J. Wen, Y. Zhang, and M. Xiao, Adv. Opt. Photonics **5**, 83 (2013).
[5] J. M. Cowley, *Diffraction Physics* (North-Holland, Amsterdam, 1995).
[6] M. V. Berry and S. Klein, J. Mod. Opt. **43**, 2139 (1996).
[7] R. Iwanow, D. A. May-Arrioja, D. N. Christodoulides, G. I. Stegeman, Y. Min, and W. Sohler, Phys. Rev. Lett. **95**, 053902 (2005).
[8] F. Pfeiffer, T. Weitkamp, O. Bunk, and C. David, Nat. Phys. **2**, 258 (2006).
[9] B. J. McMorran and A. D. Cronin, New J. Phys. **11**, 033021 (2009).
[10] M. R. Dennis, N. I. Zheludev, and F. Javier Garcia de Abajo, Opt. Express **15**, 9692 (2007).
[11] Y. Zhang, J.-M. Wen, S. N. Zhu, and M. Xiao, Phys. Rev. Lett. **104**, 183901 (2010).
[12] L. Deng, E. W. Hagley, J. Denschlag, J. E. Simsarian, M. Edwards, C. W. Clark, K. Helmerson, S. L. Rolston, and W. D. Phillips, Phys. Rev. Lett. **83**, 5407 (1999).
[13] H. Guillet de Chatellus, E. Lacot, W. Glastre, O. Jacquin, and O. Hugon, Phys. Rev. A **88**, 033828 (2013).
[14] M. V. Berry, I. Marzoli, and W. P. Schleich, Phys. World **14**, 39 (2001).
[15] X. -B. Song, H. B. Wang, J. Xiong, K. Wang, X. Zhang, K.-H. Luo, and L.-A. Wu, Phys. Rev. Lett. **107**, 033902 (2011).
[16] J. Azaña and M. A. Muriel, IEEE J. Sel. Top. Quantum Electron. **7**, 728 (2001).
[17] J. W. Goodman, *Introduction to Fourier Optics* (Roberts and Company, Englewood, CO, 2005), 3rd ed.
[18] Ideally, $g(x) \to \delta(x)$. In practice, the specific condition that must be satisfied by the grating aperture extension is much less restrictive, depending on the phase curvature of the illumination beam and grating period. The derivation of this specific condition is beyond the scope of the present Letter.